The Journal of Experimental Biology 200, 1919–1929 (1997)
Printed in Great Britain © The Company of Biologists Limited 1997
JEB0973

THREE-DIMENSIONAL KINEMATICS AND LIMB KINETIC ENERGY OF RUNNING COCKROACHES

R. KRAM*, B. WONG AND R. J. FULL

Department of Integrative Biology, University of California at Berkeley, Berkeley, CA 94720-3140, USA

Accepted 23 April 1997

Summary

We tested the hypothesis that fast-running hexapeds must generate high levels of kinetic energy to cycle their limbs rapidly compared with bipeds and quadrupeds. We used high-speed video analysis to determine the three-dimensional movements of the limbs and bodies of cockroaches (*Blaberus discoidalis*) running on a motorized treadmill at 21 cm s^{-1} using an alternating tripod gait. We combined these kinematic data with morphological data to calculate the mechanical energy produced to move the limbs relative to the overall center of mass and the mechanical energy generated to rotate the body (head + thorax + abdomen) about the overall center of mass. The kinetic energy involved in moving the limbs was 8 μJ $stride^{-1}$ (a power output of 21 mW kg^{-1}), which was only approximately 13 % of the external mechanical energy generated to lift and accelerate the overall center of mass at this speed. Pitch, yaw and roll rotational movements of the body were modest (less than ±7 °), and the mechanical energy required for these rotations was surprisingly small (1.7 μJ $stride^{-1}$ for pitch, 0.5 μJ $stride^{-1}$ for yaw and 0.4 μJ $stride^{-1}$ for roll) as was the power (4.2, 1.2 and 1.1 mW kg^{-1}, respectively). Compared at the same absolute forward speed, the mass-specific kinetic energy generated by the trotting hexaped to swing its limbs was approximately half of that predicted from data on much larger two- and four-legged animals. Compared at an equivalent speed (mid-trotting speed), limb kinetic energy was a smaller fraction of total mechanical energy for cockroaches than for large bipedal runners and hoppers and for quadrupedal trotters. Cockroaches operate at relatively high stride frequencies, but distribute ground reaction forces over a greater number of relatively small legs. The relatively small leg mass and inertia of hexapeds may allow relatively high leg cycling frequencies without exceptionally high internal mechanical energy generation.

Key words: locomotion, biomechanics, insects, arthropods, cockroach, running, *Blaberus discoidalis*.

Introduction

Two-, four-, six- and eight-legged animals accelerate and decelerate their bodies in similar ways during constant average-speed terrestrial locomotion as they move like inverted pendulums and bouncing spring-mass systems (Cavagna *et al.* 1977; Full, 1989). The external mechanical energy generated to move the body or center of mass a unit distance is directly proportional to body mass for legged animals that range in mass from a 1 g cockroach to a 73 kg ram (Full and Tu, 1991; Heglund *et al.* 1982*a*). The mass-specific mechanical energy generated to move the center of mass of six-legged insects and eight-legged crabs a unit distance is comparable with that of two- and four-legged mammals (1 J kg^{-1} m^{-1}; Blickhan and Full, 1987; Full and Tu, 1991). Thus, mass-specific mechanical energy produced to move the center of mass appears to be relatively independent of leg number, body mass, body shape and the type of skeleton being used.

Perhaps the effects of morphological diversity are not reflected in the energy generated to move the center of mass (external energy), but instead are seen in the energy produced to swing the limbs and to rotate the body (internal energy). Fedak *et al.* (1982) measured the internal mechanical power for a variety of running animals and found no systematic difference in internal power between bipedal running birds and quadrupedal mammals. A comparison of internal and external mechanical power shows clearly that internal mechanical power generation is the smaller of the two in running mammals and birds (Heglund *et al.* 1982*b*). However, the situation may be quite different in running arthropods. On the basis of data for the time of leg protraction seen in insect locomotion, Gray (1968) suggested that 'most of the energy used when (an arthropod) is travelling at a high constant speed is that required to protract the limb, the limiting factor for speed being the intrinsic power of the protractor muscles' (p. 329). Compared with mammals and birds, running arthropods move their limbs much more rapidly and often through different planes (primarily horizontal and lateral rather than sagittal). Thus, predictions for the internal mechanical energy produced by

*e-mail: rkram@socrates.berkeley.edu.

running arthropods based on data from mammals and birds seem tenuous at best. The purpose of this study was to test Gray's contention that the limb movements of rapid-running insects require the generation of substantially more mechanical power than that produced to move the center of mass or produced by other species that swing their limbs and rotate their bodies.

A mechanical model of how the legs of running animals act as springs presents an alternative hypothesis (Blickhan and Full, 1993). Running by legged animals has been modeled using a bouncing monopode or spring-mass system similar to a pogo stick (Blickhan, 1989; Cavagna *et al.* 1977; McMahon and Cheng, 1990). A single, virtual leg-spring model has been shown to be robust in its in ability to predict the mechanics of locomotion in species that differ both in actual leg number and in morphology (Blickhan and Full, 1993), as well as in animal mass (Farley *et al.* 1993). A virtual leg-spring consists of three legs for an insect using an alternating tripod gait, two legs for a trotting quadrupedal mammal and one leg for a bipedal runner. Blickhan and Full (1993) found that the relative stiffness of individual legs is remarkably similar in trotters (insects, crabs, dogs and rams), runners (birds and humans) and hoppers (kangaroo rats, springhares and kangaroos). Comparable relative individual leg stiffness appears to be attained by simply distributing the ground reaction forces among a larger number of legs. Indeed, we know from empirical data that trotting cockroaches generate one-third of their total vertical ground reaction force with each leg (Full *et al.* 1991). Distributing the forces among more legs would seem to allow each individual leg to be less robust and hence lighter. This could result in a nearly equal amount of internal mechanical energy required to swing the legs in animals that differ in leg number. A hexapedal trotter and bipedal runner would generate the same internal mechanical energy to swing their limbs if the mass and inertia of each of the hexaped's legs was one-third of that of a biped's, providing that both animals were moving at the same relative stride frequency and speed.

In the present study, we tested these hypotheses concerning how internal mechanical energy varies with body size, leg number and morphology by determining the morphometrics, three-dimensional kinematics and mechanical energy involved in moving the legs of six-legged running cockroaches. We then compared these values with those for two-legged runners and hoppers and four-legged trotters. We chose to study the death-head cockroach *Blaberus discoidalis* because of the wealth of data already available on its locomotion biomechanics (Full *et al.* 1991, 1993, 1995; Full and Tu, 1990; Ting *et al.* 1994).

Materials and methods

Animals

Cockroaches [*Blaberus discoidalis* (Serville)] were obtained from the Carolina Biological Supply Company. Kinematic data were obtained for five animals (mass 2.67±0.28 g, mean ± S.D.). Another group of similarly sized cockroaches was used to determine the center of mass locations and moments of inertia (N=5, mass 2.59±0.04 g, mean ± S.D.). Animals were housed in plastic containers and given dog chow and water *ad libitum.*

Treadmill

To conduct this study, we first had to construct a unique transparent treadmill that allowed us a ventral view of the running animal. Because of their orientation, it is impossible to view the coxa–body and coxa–femur angles from other views. The treadmill frame was made of clear Plexiglas and had a belt made from transparent acetate. This allowed an unobstructed ventral view of the animal. An open-bottomed acrylic box (14 cm×8 cm) was held loosely over the animal to enclose and direct it. A series of points painted along one edge of the belt provided reference points. The treadmill was powered by a variable-speed electric motor.

Three-dimensional video analysis system

The limb movements of running insects are rapid, and the limbs move through more than one plane. Thus, to quantify the motion accurately, a high image sampling rate and three-dimensional kinematic techniques are necessary. Video images were captured at 1000 frames s^{-1} using two cameras (a Kodak EktaPro Intensified Imager and a Kodak EktaPro SE Imager). The cameras were synchronized to capture two different views of the cockroach simultaneously, each of which filled half of the video field. The images were recorded with a Kodak EktaPro TR and then downloaded to S-VHS tapes for analysis. The cameras were positioned ventral and lateral to the animal as it ran on the treadmill. One camera was positioned to the left lateral side and the other to the right lateral side so that the angle between the optical axes of the cameras was nearly 90 °. This maximized three-dimensional position accuracy.

Prior to each run, a stationary calibration object was placed in the space where the animal would run to allow three-dimensional calibration of the field of view. The calibration object had overall dimensions of approximately 2.5 cm×2.5 cm×1.0 cm and had eight points of known coordinates distributed onto two different horizontal planes. The object was made from small plastic blocks (LEGO Systems Inc.), which we measured with electronic digital calipers (resolution 0.01 mm; Omega Scientific Co.). A rectangular coordinate system was established with the positive x-axis directed horizontally and laterally towards the right of the animal, the positive y-axis directed horizontally and anteriorly, and the z-axis directed vertically with its positive end pointing dorsally (Fig. 1). This is the same sign convention used by Full *et al.* (1991).

To aid in digitizing, 32 points, corresponding to joint centers and other anatomical landmarks were marked on the ventral side of the cockroach with white epoxy paint (Duro Appliance). The points are shown in Fig. 1. One complete stride was analyzed for each animal. We selected strides for analysis where the animal exhibited straight-ahead running at a nearly constant speed of approximately 20 cm s^{-1} using an

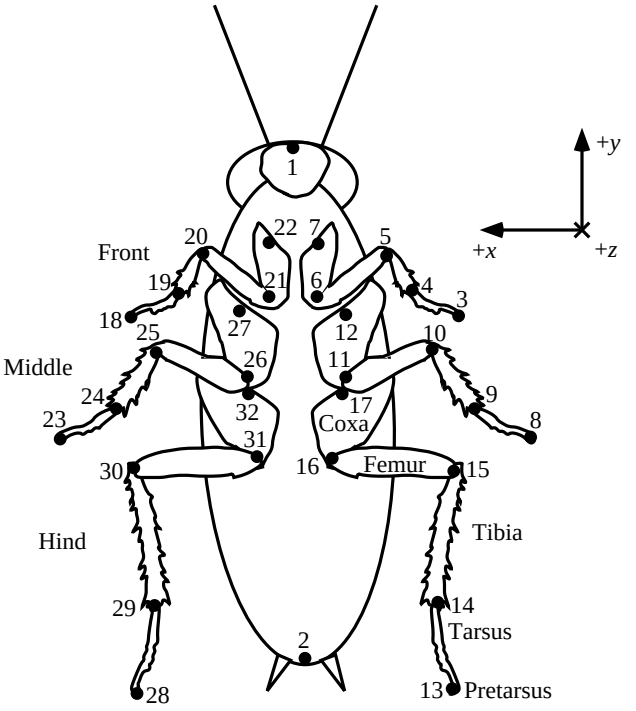

Fig. 1. Ventral view of the cockroach *Blaberus discoidalis* showing points that were marked and digitized. Note also our convention for *x*, *y* and *z* coordinates. Points 1 and 2 define the longitudinal axis. The *z*-axis is directed vertically with its positive end pointing dorsally. Points 3, 8, 13, 18, 23 and 28 are the pre-tarsal claws. Points 4, 9, 14, 19, 24 and 29 are the tibia–tarsal joints. Points 5, 10, 15, 20, 25 and 30 are the femur–tibia joints. Points 6, 11, 16, 21, 26 and 31 are the coxa–femur joints. Points 7, 12, 17, 22, 27 and 32 are the coxa–body joints.

alternating tripod gait. We digitized the video images to obtain the coordinates of the 32 points, along with two reference points on the treadmill belt for each field from both camera views. The raw coordinate data were filtered using a low-pass, fourth-order, zero-phase-shift Butterworth digital filter with a cut-off frequency of 25 Hz. Three-dimensional coordinates were calculated by the direct linear transformation method (Biewener and Full, 1992) using a computer software package (Peak Performance Technologies Inc.).

The resolution of the video images averaged 0.33 mm per pixel. We were able to locate the *x*, *y* and *z* coordinates of a point in space with mean squared errors of 0.052 mm, 0.053 mm and 0.070 mm for the *x*, *y* and *z* directions, respectively. This gave a combined mean squared error for position of 0.107 mm.

Body and limb segment moments of inertia

To determine the mass moments of inertia of the body, animals were killed and then deep-frozen. 'Body' here refers to the head, thorax and abdomen (HTA), in other words, the whole animal minus the legs. Each frozen cockroach body (HTA) was skewered with a pin which was supported by two parallel razor blade edges. This allowed the HTA to swing freely with negligible friction. The HTA was tapped lightly, and the period of oscillation measured from high-speed video tapes of the swinging. Knowing this period, the mass and the location of the pin axis relative to the HTA center of mass was sufficient to calculate the moments of inertia using the parallel axis theorem (Beer and Johnston, 1977; Blickhan and Full, 1992). This swinging procedure was performed for all three axes. The center of mass of the HTA was located by finding where it balanced on a razor blade edge and assuming bilateral symmetry. The lengths of the limb segments were measured directly with electronic digital calipers. Segments were weighed with an electronic balance (Mettler AE50) to the nearest 0.0001 g. To estimate the moment of inertia (I) about their center of mass, the coxae of the middle and hind legs were approximated as right-angled triangular plates of uniform density. We used the equation:

$$I = \frac{1}{18}\, mh^2 , \tag{1}$$

where h is the height of the right-angled triangular plate and m is the mass of the segment. All other segment moments of inertia were approximated as slender rods of uniform density using the equation:

$$I = \frac{1}{12}\, ml^2 , \tag{2}$$

where l is the length of the segment.

Pitching angle was calculated from the z coordinates of the head and abdomen points. Our convention is that a positive pitch angle indicates that the head is above the abdomen. Roll was calculated from the z coordinate of the hind leg coxa. A positive roll angle indicates that the left side of the body is higher. Yaw was calculated from the x and y coordinates of the head and tail points. A positive yaw angle indicates a turn to the left. Rotational kinetic energies (RKE_{HTA}) were calculated knowing the appropriate moment of inertia, I, and the angular velocity, ω, using the equation:

$$RKE_{HTA} = \frac{1}{2}\, I\omega^2 . \tag{3}$$

The total internal mechanical energy for each limb segment had three components. The translational kinetic energy (TKE) relative to the overall center of mass was calculated from segment mass (m) and the resultant velocity (v) of the segment center of mass relative to the overall animal center of mass, using the equation:

$$TKE = \frac{1}{2}\, mv^2 . \tag{4}$$

The overall animal center of mass was calculated using Peak-5 software (Peak Performance Technologies Inc.) for each frame and incorporated the HTA center of mass and each limb segment center of mass. The rotational kinetic energy of each segment ($RKE_{segment}$) was calculated from its inertia about its

center of mass (I), and the angular velocity (ω) of that segment in a global coordinate system using the equation:

$$\mathrm{RKE}_{\mathrm{segment}} = \frac{1}{2} I\omega^2 . \quad (5)$$

The third component of the internal mechanical energy of the limbs is gravitational potential energy. If a single limb is raised alone, this change in gravitational potential energy will be detected by a force platform that measures ground reaction forces, and this has already been measured (Full and Tu, 1990). However, if a limb is raised while its counterpart on the other side is lowered, a force platform will detect no change in gravitational potential energy. To measure these reciprocating vertical movements, we first calculated the changes in the height of each leg segment relative to the ground (i.e. absolute). We then calculated the sum of each of these curves at each interval in time. This first calculation provides data equivalent to a force platform record, which we refer to as the minimum gravitational work. Next, we calculated the sum of the increments for each segment and then summed these increments. This provides a value for the maximum gravitational work. The difference between these two values is equal to the internal work done against gravity while making reciprocating vertical movements of the leg pairs. It has been demonstrated that, in large mammals (e.g. humans), the gravitational potential energy involved in reciprocating leg movements is small (Cavagna and Kaneko, 1977; Willems *et al.* 1995) and it is often ignored (Fedak *et al.* 1982). In order to make comparisons among animals, we have calculated the gravitational potential energy involved in reciprocating limb movements separately from limb kinetic energies.

In many locomotor movements, mechanical energy is converted between different types of energy and transferred from one segment to another. For example, as a limb is allowed to lower, gravitational potential energy is converted into kinetic energy. It is also relatively easy to visualize how kinetic energy can flow from proximal to distal segments during whip-like movements. However, transfer of internal mechanical energy within and between segments remains a controversial and unresolved issue in biomechanics (Williams and Cavanagh, 1983; Martin *et al.* 1993). We have calculated the limb kinetic energy in several ways: no transfer, complete transfer within and between segments and limbs, and assuming transfer only within each limb. In this way, we have bounded the measurement so that we can test our hypotheses and make comparisons with data collected by others on different species.

Terminology

A step refers to half of a complete stride cycle. The contact phase refers to the time when some part of a leg is in contact with the ground, as opposed to the swing phase when the leg is not in contact with the ground. Extension refers to an increase in the internal angle between two limb segments. Flexion refers to a decrease in this internal angle.

Determination of body (HTA) axis

Because it allowed accurate digitizing, we initially defined the body axis of the insect as the segment connecting two points: the head and the most posterior point of the abdomen. However, this axis did not pass through the center of mass of the HTA (head + thorax + abdomen). To facilitate measurements and calculations, we adjusted the axis so that it passed through the center of mass of the HTA. To locate the center of mass of the HTA, we suspended the HTA vertically by a pin inserted laterally through the posterior end of the abdomen and considered the lateral (y,z) view. A small weight was hung from a thread tied onto the pin to indicate true vertical on the video images. This vertical defined a line (running anterior to posterior) along which the center of mass must lie. We determined the location along the longitudinal axis by balancing the frozen HTA on a thin support. We used the intersection of these two lines to indicate the position of the center of mass of the HTA in the lateral (y,z) plane of the animal. We used an image analysis program (NIH Image version 1.4.1) to analyze video-taped images of these procedures. On the basis of this information, we adjusted the z coordinate of the head point so that the head–tail axis connected the adjusted head point, the abdomen point and the center of mass of the HTA. This adjustment raised the z coordinate of the head by approximately 4 mm.

Results

Limb and body dimensions

Table 1 summarizes the length, mass and moment of inertia of the limb segments and the body. The mean body length (from head to tip of abdomen) was 44.1±0.8 mm and the center of mass of the HTA was located along the midline 24.0±0.6 mm posterior to the front edge of the head or 54.4 % of the length of the animal.

Speed and stride kinematics

The mean forward speed for the five individual runs analyzed was 21.0±2.3 cm s^{-1} (mean ± S.E.M.). Throughout this Results section, mean values are followed by the standard error of the mean (S.E.M.). Force platform recordings have shown that, at this speed, *B. discoidalis* uses a bouncing gait in which the overall center of mass is at its lowest point during the middle of a contact phase (Full and Tu, 1990). Thus, this gait is analogous to a quadrupedal trot. The mean stride frequency was 6.77±0.79 Hz, which translates into a mean stride length of 3.12±0.25 cm. The mean duty factors (i.e. the fraction of the stride when the foot is in contact with the ground) were 0.53±.03 for the front leg, 0.56±.03 for the middle leg and 0.53±0.12 for the hind leg.

Kinematic data set

Our complete kinematic data set is too large to include in this publication. In this section, we highlight the important features of the leg movements and do so on a leg-by-leg basis. Leg angle data are presented in Fig. 2 and Table 2.

Table 1. *Segment length, segment mass and moment of inertia about the segment center of mass for* Blaberus discoidalis

Segment	Length (m)	Mass (kg)	Moment of inertia ($kg\,m^2$)	
Front leg				
Coxa	7.20×10^{-3} ($\pm0.24\times10^{-3}$)	2.0×10^{-5} ($\pm0.1\times10^{-5}$)	8.8×10^{-11} ($\pm1.0\times10^{-11}$)	
Femur	7.65×10^{-3} ($\pm0.20\times10^{-3}$)	7.9×10^{-6} ($\pm0.4\times10^{-6}$)	3.9×10^{-11} ($\pm0.3\times10^{-11}$)	
Tibia	4.18×10^{-3} ($\pm0.23\times10^{-3}$)	2.9×10^{-6} ($\pm0.1\times10^{-6}$)	4.1×10^{-12} ($\pm0.4\times10^{-12}$)	
Tarsus and pretarsus	5.39×10^{-3} ($\pm0.14\times10^{-3}$)	1.6×10^{-6} ($\pm0.1\times10^{-6}$)	3.5×10^{-12} ($\pm0.3\times10^{-12}$)	
Middle leg				
Coxa	5.77×10^{-3} ($\pm0.16\times10^{-3}$)	3.8×10^{-5} ($\pm0.3\times10^{-5}$)	5.8×10^{-11} ($\pm0.4\times10^{-11}$)	
Femur	9.86×10^{-3} ($\pm0.35\times10^{-3}$)	1.4×10^{-5} ($\pm0.1\times10^{-5}$)	1.2×10^{-10} ($\pm0.1\times10^{-10}$)	
Tibia	7.70×10^{-3} ($\pm0.47\times10^{-3}$)	6.6×10^{-6} ($\pm0.3\times10^{-6}$)	3.4×10^{-11} ($\pm0.4\times10^{-11}$)	
Tarsus and pretarsus	6.58×10^{-3} ($\pm0.27\times10^{-3}$)	2.1×10^{-6} ($\pm0.3\times10^{-6}$)	7.5×10^{-12} ($\pm0.9\times10^{-12}$)	
Hind leg				
Coxa	6.08×10^{-3} ($\pm0.30\times10^{-3}$)	4.8×10^{-5} ($\pm0.3\times10^{-5}$)	8.1×10^{-11} ($\pm0.4\times10^{-11}$)	
Femur	1.06×10^{-2} ($\pm0.03\times10^{-2}$)	1.8×10^{-5} ($\pm0.1\times10^{-5}$)	1.7×10^{-10} ($\pm0.1\times10^{-10}$)	
Tibia	1.28×10^{-2} ($\pm0.04\times10^{-2}$)	1.1×10^{-5} ($<\pm0.1\times10^{-5}$)	1.5×10^{-10} ($\pm0.1\times10^{-10}$)	
Tarsus and pretarsus	8.02×10^{-3} ($\pm0.38\times10^{-3}$)	2.6×10^{-6} ($\pm0.1\times10^{-6}$)	1.4×10^{-11} ($\pm0.1\times10^{-11}$)	
Body (legs excluded)	4.41×10^{-2} ($\pm0.11\times10^{-2}$)	2.25×10^{-3} ($\pm0.03\times10^{-3}$)	1.86×10^{-7} ($\pm0.13\times10^{-7}$)	Pitch
			2.04×10^{-7} ($\pm0.04\times10^{-7}$)	Yaw
			1.93×10^{-8} ($\pm0.37\times10^{-8}$)	Roll

Body includes head, thorax and abdomen, but excludes all leg segments.

Values are means for five animals, with (±S.D.).

Table 2. *Joint angle changes during the contact phase*

Joint angle (degrees)	Hind leg	Middle leg	Front leg
Body–coxa			
Initial	26.6 (±4.7)	40.9 (±6.7)	69.2 (±13.7)
Final	18.5 (±1.3)	27.8 (±3.3)	35.3 (±10.0)
Range	–8.1 (±4.5)	–13.1 (±4.3)	–33.9 (±6.5)
Coxa–femur			
Initial	35.7 (±10.1)	43.5 (±10.1)	62.4 (±8.6)
Final	105.9 (±11.6)	86.5 (±7.7)	71.1 (±10.4)
Range	+70.2 (±3.6)	+43.0 (±7.5)	+8.6 (±14.2)
Femur–tibia			
Initial	52.2 (±4.5)	81.3 (±9.9)	114.6 (±4.7)
Final	120.2 (±8.7)	107.5 (±2.6)	90.7 (±16.9)
Range	+67.9 (±5.6)	+26.2 (±11.1)	–23.8 (±18.2)

Body–coxa angle is the projected angle in the *y*,*z* (sagittal) plane.

Values are means (±S.D) (N=5).

A negative range indicates flexion and a positive range indicates extension.

Hind leg

The most proximal joint is the body–coxa joint. The axis of this joint is parallel to the *x*-axis, and it is primarily a joint with a single degree of freedom (i.e. a hinge). Thus, it is easiest to consider the angle projected onto the *y*,*z* (i.e. sagittal) plane. This angle changed by an average of only approximately 8° during the contact phase (Fig. 2A; Table 2). The coxa–femur joint of the hind leg is hinge-like with its axis parallel to the *z*-axis. In contrast with the body–coxa joint, the coxa–femur joint extended over 70° during the contact phase (Fig. 2B). The femur–tibia joint of the hind leg is also hinge-like with an axis parallel to the *z*-axis. It too exhibited substantial extension (almost 70°) during the power stroke (Fig. 2C).

Middle leg

The orientations of the joints of the middle leg were similar to those of the hind leg. The *y*,*z* projection of middle leg coxa–body angle changed by 13° during the contact phase, a much larger change than in the hind leg (Fig. 2D; Table 2). As in the hind leg, the coxa–femur joint of the middle leg exhibited substantial (approximately 43°) extension during the contact phase (Fig. 2E). The femur–tibia joint of the middle leg was hinge-like with an axis parallel to the *z*-axis. This joint extended moderately during the contact phase, approximately 26° on average (Fig. 2F).

Front leg

The anatomy and joint orientation of the front legs were quite different from those of the middle and hind legs. The body–coxa joint of the front leg is not a pure hinge joint, but during locomotion the coxa segment moved primarily in the sagittal plane as though the joint axis were nearly parallel to the *x*-axis, as for the middle and hind legs. However, relative to the middle and hind legs, the body–coxa angle of the front leg exhibited the largest angular excursion during the contact phase, approximately 34° (Fig. 2G). This is more than four times the excursion of the hind leg body–coxa joint. The coxa segment of the front leg is itself quite different from the coxae of the middle and hind legs (Fig. 1; Table 1). The front leg coxa is a relatively long and slender rod shape, but the

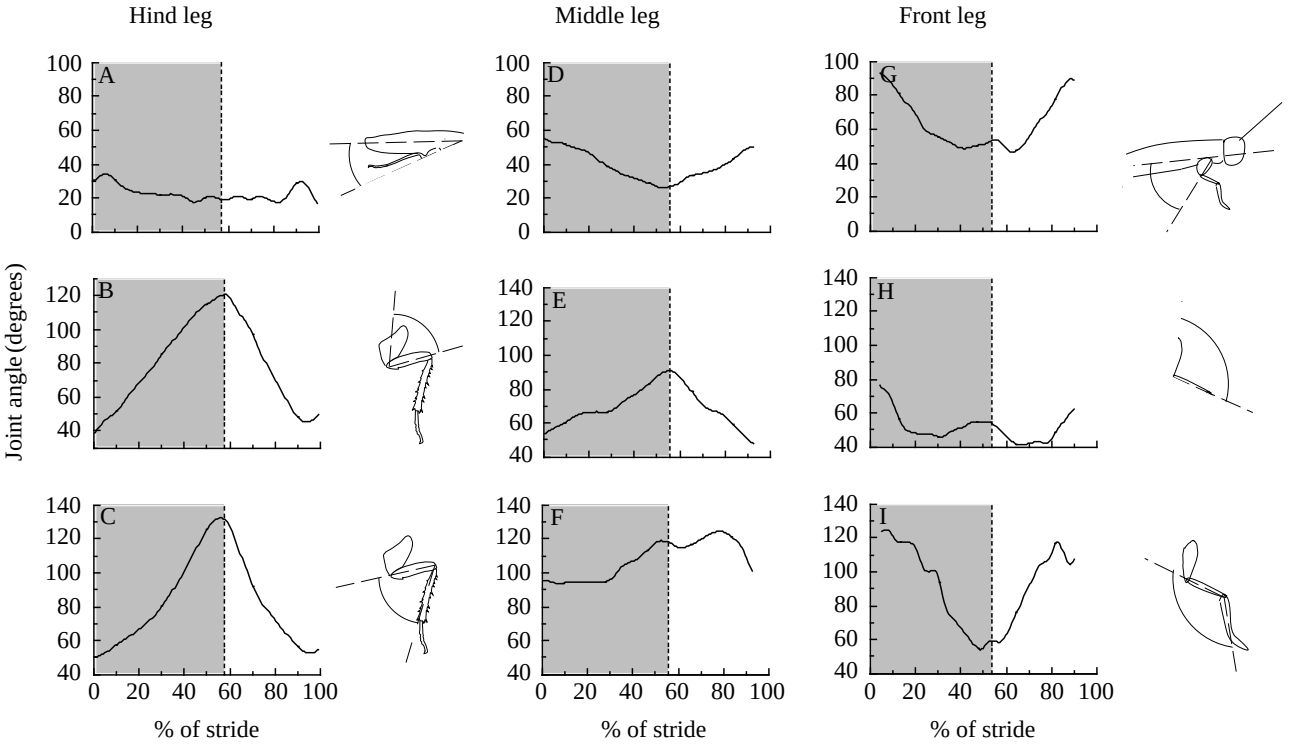

Fig. 2. Major joint angles for hind (A,B,C) and middle (D,E,F) and front (G,H,I) legs during one stride. These data and Fig. 3 are from a set of legs that act together in a tripod. The shaded area represents the ground contact (stance) phase. The projected coxa–body angles (*y*,*z* plane) changed relatively little over the contact phase in the hind and middle legs (A,D) but swept a sizable arc in the front leg (G) (approximately four times greater than that in the hind leg). The coxa–femur joints extended steadily (in the *x*,*y* plane) and substantially during the contact phase in the hind and middle legs (B,E), in contrast with the coxa–femur net angular excursion in the front leg (H). Note also that the femur–tibia angle extends during contact in the middle and hind legs (C,F) (predominantly in the *x*,*y* plane), but flexes in the front leg (I) (mostly in the *y*,*z* plane). Angular movement at the femur–tibia joint of the front legs during the contact phase was quite variable from stride to stride, but generally exhibited flexion.

middle and hind leg coxae are shaped like stout triangular wedges.

The coxa–femur joint of the front leg is a hinge joint, and during locomotion its axis is parallel to the *x*-axis, unlike the axes of the middle and hind legs. Thus, the femur of the front leg moves in more of a sagittal plane (*y*,*z*), while most of the femur movement in the middle and hind legs takes place in the *x*,*y* plane. The movements of the coxa–femur joint of the front leg were more variable than those of the middle and hind legs. There was no large net angular excursion during contact (average only approximately 9 °; Fig. 2H). The variability is obvious from Table 2 and, although the mean angular excursion was a small extension, almost as many trials exhibited a slight flexion movement.

The femur–tibia joint of the front leg is hinge-like with an axis parallel to the *x*-axis; again unlike the middle and hind legs. The angular excursion pattern during the contact phase was generally moderate flexion (Fig. 2I), but there was also considerable variability from step to step and between animals (Table 2).

Body (HTA) rotations

The pitching, yawing and rolling movements were more variable than the limb movements. We anticipated that there would be two pitching movements per stride cycle and, while this was generally the case (see Fig. 3), some trials only showed one cycle. The head and abdomen had vertical amplitudes of more than 5 mm (180 ° out of phase). The downward pitching of the head usually occurred just after the beginning of the contact phase of each step. The head/abdomen displacements translate to a pitching angle amplitude of approximately ±5 °.

During straight-ahead running, there was typically one cycle of yawing per stride (Fig. 3). The amplitude of yawing was small, less than ±4 °. The head moved laterally towards the side which had the middle leg on the ground, while the abdomen moved in the opposite direction.

There were usually two rolling movements per stride. Early in the support phase of each tripod, the HTA rolled towards the side with two legs in contact with the ground, reaching a maximum roll angle of approximately 7 °. As the step progressed, the HTA rolled back to a neutral attitude and then, with the initiation of the next step, rolled in the opposite direction.

Limb mechanical energies

We calculated the kinetic energy for moving the limbs (TKE

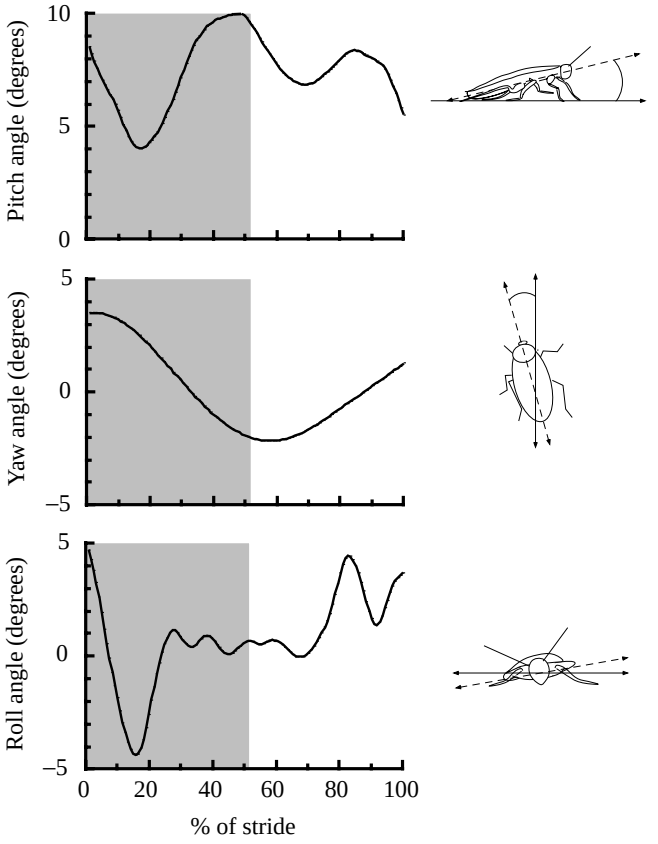

Fig. 3. Rotational movements of the head + thorax + abdomen (HTA) about its center of mass during a stride. Note that (A) pitch, (B) yaw and (C) roll angles were all small (less than ±7 °) compared with most leg angle changes. The shaded area represents the ground contact (stance) phase.

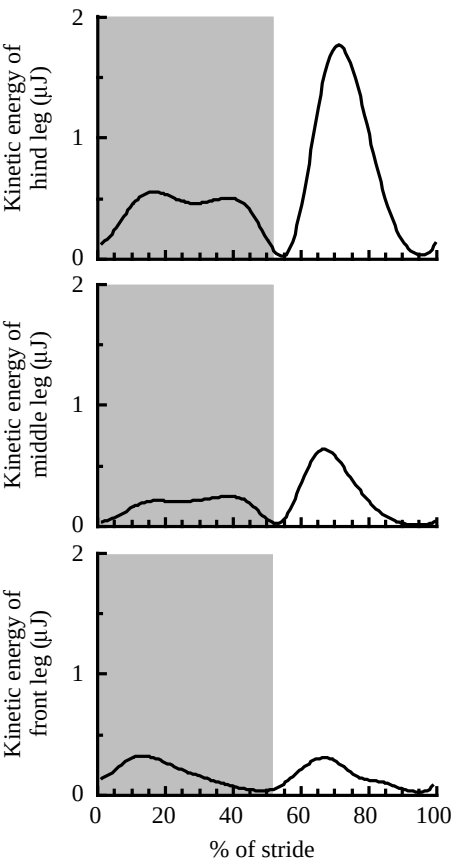

Fig. 4. Limb kinetic energy fluctuations for a running *Blaberus discoidalis* for the hind, middle and front legs. Values for a front, middle and hind leg from a tripod are plotted here. The vast majority of the increases in kinetic energy occurred during the initiation of the swing phase, i.e. at the beginning of the second half of the stride depicted here. The shaded area represents the ground contact (stance) phase.

+ RKE) using three assumptions about transfer of mechanical energy: no transfer (8.72±0.90 μJ stride^{-1}), transfer within each limb but not between limbs (8.24±0.86 μJ stride^{-1}) and transfer within and between limbs (6.86±0.81 μJ stride^{-1}). We agree with Fedak *et al.* (1982) that the assumption of transfer within but not between limbs is the most reasonable. Thus, our value of 8.24 μJ stride^{-1} or 20.9 mW kg^{-1} can be compared with the values reported by Fedak *et al.* (1992) for other species. Considered separately, the rotational kinetic energies were less than one-tenth of the magnitude of the translational kinetic energies.

As shown in Fig. 4, almost all of the increases in limb kinetic energy occurred during the swing phase. At the end of the contact phase, the leg translational velocities relative to the overall center of mass and the angular velocities all slow. The vertical position of the leg did not change substantially during the contact phase. As a result, there was a brief decline in the energy level at the end of the contact phase. Then, during swing, each leg was lifted vertically and swung rapidly forward. There is an obvious increase to a peak value in the kinetic energy level for each leg during the swing phase. Note that, in Fig. 4, a tripod of legs is plotted so that the contact and swing phases are registered. Thus, the middle leg depicted is from the opposite side from the front and middle legs.

The gravitational potential energy needed for the reciprocal vertical movements of the limbs was 3.10±0.27 μJ stride^{-1}. It seems unlikely that this mechanical energy could be reduced by transfer of kinetic energy within limbs. In running cockroaches (unlike cursorial mammals and birds), the kinetic energy of the limbs is the result of movements in the plane parallel to the ground, and thus it seems difficult to transfer this into vertical movements against gravity. In addition, the limbs are lifted at the end of the contact phase when the limb kinetic energy is near zero. Thus, compared with the limb kinetic energy, the gravitational potential energy required for reciprocal vertical limb movements is not negligible in running cockroaches.

Body (HTA) mechanical energies

All of the body (HTA) rotational kinetic energy fluctuations were small relative to the gravitational potential and forward kinetic energy fluctuations of the overall center of mass. The

largest was the pitching kinetic energy. The mean sum of positive increases was $1.66\pm0.18\,\mu J\,stride^{-1}$ ($4.22\pm0.46\,mW\,kg^{-1}$) for pitching, $0.46\pm0.03\,\mu J\,stride^{-1}$ ($1.17\pm0.08\,mW\,kg^{-1}$) for yawing and $0.44\pm0.03\,\mu J\,stride^{-1}$ ($1.12\pm0.08\,mW\,kg^{-1}$) for rolling. Although the roll angle amplitude was sizable (approximately ±5°), the moment of inertia about the roll axis was almost exactly ten times smaller than the moment of inertia about the pitch or yaw axes.

Discussion

Limb kinetic energy

Several leg segments of the cockroach *Blaberus discoidalis* swept rapidly through large angles during running (Fig. 2). Despite the rapid movements of six legs, the translational and rotational kinetic energy involved in moving the limbs was only 13% of the external mechanical energy generated to lift and accelerate the overall center of mass (Full and Tu, 1990).

On a leg-by-leg basis, the kinetic energies reflected differences in cockroach leg morphology (Fig. 4). We calculated the kinetic energy for moving the limbs (TKE + RKE) on a leg-by-leg basis using the assumption of no energy transfer. This assumption made it possible to break down the energy further on a segment-by-segment basis and, as indicated earlier, the assumption of 0 or 100% energy transfer within a limb had relatively little effect. These calculations demonstrated that the hind legs account for approximately 56%, the middle legs for 30% and front legs for 14% of the total limb kinetic energy (Fig. 5). These percentages are roughly the same as the breakdown of leg mass among legs (see Table 1). However, on a limb-segment basis, the mechanical power was clearly not proportional to the mass of the segment. For example, in the hind leg, the coxa is almost 20 times more massive than the tarsus/pretarsus segments but the rapid movements of the tarsus/pretarsus involved more than three times as much kinetic energy. Despite the more distal segments being less massive, they move at much higher velocities. Leg length, mass and inertia were smallest for the front leg, largest for the hind legs and intermediate for the middle legs (Table 1). The kinetic energy generated to move the hind legs was more than four times that produced by the small front legs. The kinetic energy of the middle legs was just over half of that involved in moving the hind legs.

Segmental mechanical energies within a leg were not all predictable from the morphology alone. Despite the coxa being the largest segment of the middle and hind legs, only a small amount of segmental mechanical energy was generated to move these segments during running (Fig. 5). The greatest amount of segmental mechanical energy was generated to move the tibia, the second smallest segment of the middle and hind legs. Tibial mechanical energy was a result of the large and rapid angle changes at the coxa–femur and femur–tibia joints (Fig. 2). In general, the proximal concentration of segmental mass and limb musculature minimizes the mechanical energy produced to lift and swing the limbs, and this leg design also appears in many other terrestrial animals (Gray, 1968; Hildebrand, 1960). Although not explicitly stated as a design criterion, the designs of legged robots also have proximally located mechanical actuators (Angle, 1991).

Body (HTA) rotations

The head–thorax–abdomen (HTA) of the cockroach constitutes nearly 87% of the total animal mass (Table 1), and these small animals run with high stride frequencies. Thus, we hypothesized that the mechanical power produced in rotating the HTA relative to its center of mass would be substantial. Surprisingly, the combined mechanical energy generated in the pitching, yawing and rolling movements of *B. discoidalis* was only approximately 4% of the external mechanical energy generated to move the overall center of mass. Even though the

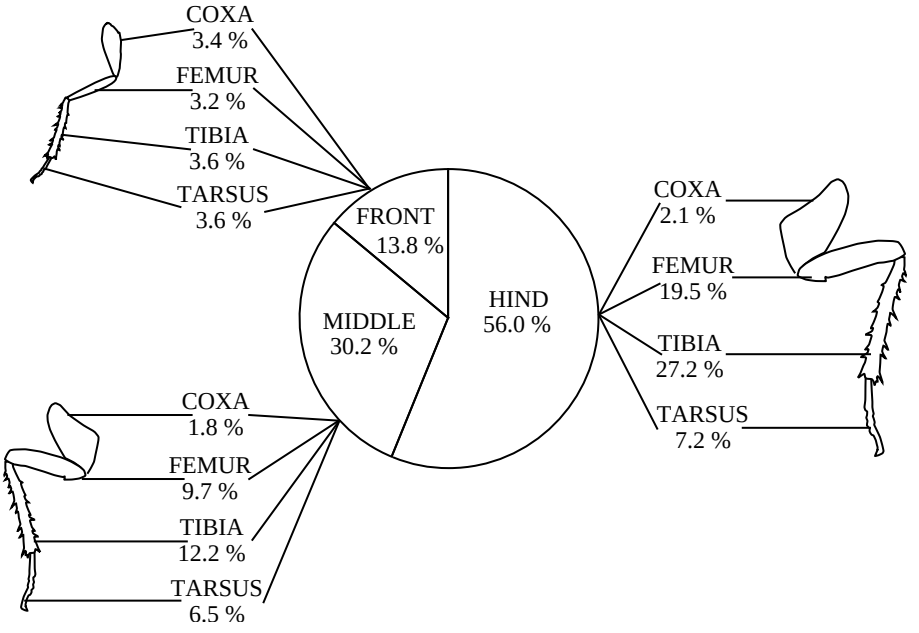

Fig. 5. Graphical summary of limb kinetic energy. More than half of all the limb kinetic energy was associated with the hind leg. Within a leg, the energy required to move the individual segments was not tightly linked to the mass of the segment. For example, the coxa of the hind leg was almost 20 times more massive than the tarsal segment but was associated with only one-third as much kinetic energy because of the much higher velocities of the more distal segments.

angular fluctuations were all small, the vertical movements of the head and abdomen points were more than 20 times larger than the vertical movements of the overall center of mass indicated from force platform measurements (Full and Tu, 1990). The pitching, yawing and rolling movements followed discernible patterns, as described in previous considerations of hexapedal stability (Ting *et al.* 1994), but were among the most variable of the movements we measured. Therefore, it is difficult to draw any conclusions concerning the control of attitude. Maintaining a constant attitude (i.e. minimal body rotations) has been used as a control parameter by many roboticists (Angle, 1991; Hirose, 1984; Okhotsimskiy *et al.* 1972) and has been suggested to be important in some slow-walking insects (Cruse, 1976). Given the variability in HTA rotations of *B. discoidalis*, it is remarkable that the overall center of mass does not experience vertical oscillations greater than a few tenths of a millimeter.

Animal size, leg number and internal mechanical energy

The mass-specific mechanical energy generated by the trotting hexapod *B. discoidalis* to swing its limbs and rotate its body (HTA) was less than that predicted from data for two-legged runners and hoppers and from four-legged trotters (Fig. 6). The regression equation for limb kinetic energy reported by Fedak *et al.* (1982) for birds and mammals, which assumes complete energy transfer within segments in the same leg, extrapolates to $41\,mW\,kg^{-1}$ for an animal moving at $20\,cm\,s^{-1}$ regardless of size. Our mean value for limb kinetic energy for the cockroach, $20.9\,mW\,kg^{-1}$, is approximately half of this predicted value. However, considering the large differences in size and the variability about the predicted line, it is remarkably similar.

Although it is possible to compare small and large animals at the same absolute speed, it is sometimes preferable to compare animals at 'physiologically equivalent speeds'. One definition of a physiologically equivalent speed is the speed at which animals use the same gait. It is instructive to compare the mechanical energy production of running cockroaches with that of other much larger animals at the physiologically equivalent mid-trot speed. It is convenient to use the regression equations of Heglund *et al.* (1982*b*) for internal and external mechanical power for this comparison. For a 100 kg animal, roughly the size of a pony, the mid-trot speed would be approximately $3\,m\,s^{-1}$ and at that speed internal power is approximately 33 % of the total mechanical power. For a dog-sized animal, the mid-trot speed would be approximately $2\,m\,s^{-1}$ and at that speed internal power would be approximately 27 % of the total mechanical power. A speed of $20\,cm\,s^{-1}$ is a mid-trotting speed for a cockroach. At this speed, we found that the mean rate of limb kinetic energy required is only approximately 13 % of the mechanical power required to lift and accelerate the overall center of mass (external mechanical power).

Despite their rapid leg movements, six-legged cockroaches generated a mass-specific internal mechanical energy comparable with that of two-legged runners and hoppers and four-legged trotters, in part because each leg of the cockroach was relatively smaller in mass and lower in inertia than a single leg of a bird or mammal (Fig. 7). Individual legs of the cockroach were actually smaller than one-third of the mass of a biped's leg or two-thirds of the mass of a quadruped's leg, the values that would generate the same internal mechanical energy given that the animals were moving at the same relative stride frequency and speed. The tripod of legs that cockroaches use during trotting actually comprised less than one-quarter of the mass expected for one leg of bipedal runners or two legs of quadrupedal trotters of equal total body mass.

The small leg mass of cockroaches (and perhaps of insects in general) allows the legs to be operated at relatively high frequencies without increasing the internal mechanical energy. The ability of hexapods to operate at higher relative frequencies is consistent with the bouncing monopode model derived from the mechanical energy of the overall center of mass along with ground reaction forces. Blickhan and Full (1993) estimated the relative stiffness of a monopode's leg by dividing whole-animal relative force ($F/m\boldsymbol{g}$, where F is the peak ground reaction force, m is animal mass and $\boldsymbol{g}$ is the acceleration due to gravity) by the relative compression of the virtual leg-spring ($\Delta l/l$, where Δl is the compression of the virtual leg-spring and l is the monopode's leg length). Six-legged trotters (insects using three legs on the ground during a step) were discovered to compress their virtual leg-spring by

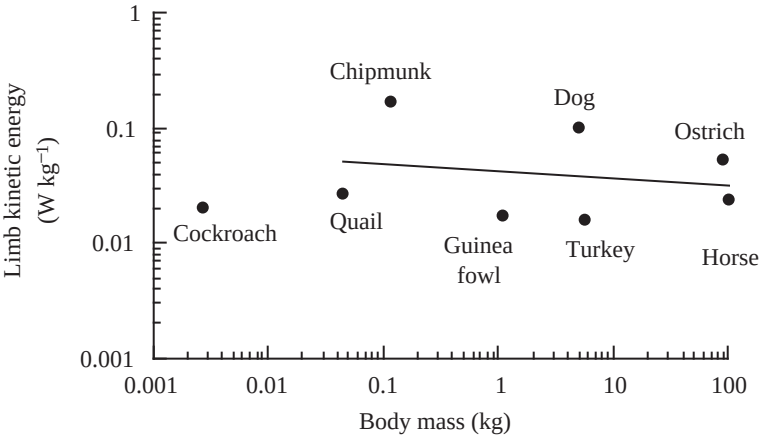

Fig. 6. Mass-specific limb kinetic energy as a function of animal mass plotted on logarithmic scales. Values are calculated using the individual species regression equations (Fedak *et al.* 1982) for animals theoretically moving at the same speed ($20\,cm\,s^{-1}$).

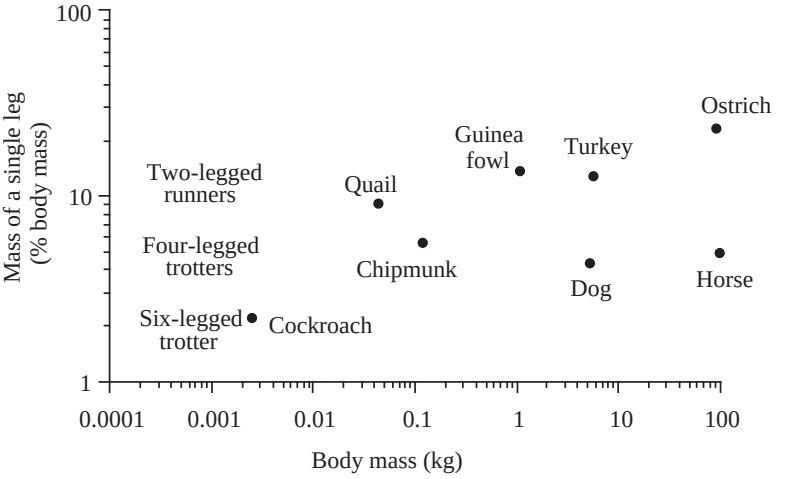

Fig. 7. Mass of a single leg as a function of animal mass for runners and trotters plotted on logarithmic scales. The leg mass of a cockroach (total mass divided by leg number) is much smaller than that predicted for a biped or quadruped of similar size. Values are taken from Fedak *et al.* (1982).

only a small amount (one-third of that of bipedal runners and hoppers). Because the whole-animal relative force produced by an insect is the same as that produced by bipedal runners, the stiffness of the insect's virtual leg-spring is three times greater than that of runners (F/mg)/($\frac{1}{3}\Delta l/l$). The relatively greater stiffness of the insect's virtual leg-spring results in a shorter distance traveled during a step along with a higher stride frequency. Three cockroach legs of comparable relative stiffness sum to produce a relatively stiff virtual leg-spring that operates at relatively high frequencies. In the present study, we found that, despite these high frequencies, the mass-specific limb kinetic energy in cockroaches is comparable to that of larger animals moving at the same absolute speed (Fig. 6). This was the result of relatively small individual leg masses (Table 1) and inertia offsetting the relatively high stride frequencies. We reject the hypothesis that limb movements in small rapid-running polypeds require the generation of substantially more mechanical power than measured in bipeds and quadrupeds.

Future directions

The present data on leg length, mass, inertia and three-dimensional kinematics provide the basic information necessary to complete our attempt at integrating whole-animal mechanics with leg and muscle function. Our laboratory has begun a detailed anatomically accurate, dynamic computer simulation of the cockroach musculoskeletal system (Full and Ahn, 1995). This model is now being extended to a realistic, whole-animal dynamic simulation of locomotion using the present data. These data make it possible to calculate the net joint moments and the net power production and absorption at each joint of each leg. This analysis of joint power will help explain how the muscles themselves must act to produce locomotion and may aid in locating the spring used during trotting (Full *et al.* 1993). A combination of our external kinematic data and the three-dimensional muscle anatomy is being used to conduct sensitivity analyses to guide our future experiments on isolated muscle.

Finally, one application of the present research is to provide engineers with a kinematic description of a running insect to use as a starting point for the design of legged robots which can run over varied terrain. At present, living animals run much faster and are more maneuverable than multi-legged robotic vehicles (Alexander, 1990; Full, 1993). However, this performance gap is narrowing (Raibert, 1990; Raibert and Hodgins, 1992). Insects have been identified as model animal systems which are likely to provide inspiration for the design of autonomous legged vehicles (Beer and Hillel, 1993; Binnard, 1992, 1995; Full, 1993; Powers, 1996). The cockroach is a particularly good model for a legged robot because its sprawled tripod posture offers high static stability at slower speeds, yet this design does not restrict rapid, dynamic locomotion at high speeds (Ting *et al.* 1994).

Supported by ONR Grant NOOO14-92-J-1250.

References

ALEXANDER, R, MCN. (1990). Three uses for springs in legged locomotion. *Int. J. Robot. Res.* **9**, 53–61.

ANGLE, C. M. (1991). Design of an artificial creature. MS thesis, Massachusetts Institute of Technology.

BEER, F. P. AND JOHNSTON, E. R. (1977). *Vector Mechanics for Engineers: Dynamics.* New York: McGraw Hill.

BEER, R. D. AND HILLEL, J. C. (1993). Simulations of cockroach locomotion and escape. In *Biological Neural Networks in Invertebrate Neuroethology and Robotics* (ed. R. D. Beer, R. E. Ritzmann and T. McKenna), pp. 267–286. Boston: Academic Press, Inc.

BIEWENER, A. A. AND FULL, R. J. (1992). Force platform and kinematic analysis. In *Biomechanics: Structures and Systems, A Practical Approach* (ed. A. A. Biewener), pp. 45–73. Oxford: IRL Press at Oxford University Press.

BINNARD, M. B. (1992). *Leg Design for a Small Walking Robot*. Cambridge, MA: MIT.

BINNARD, M. B. (1995). *Design for a Small Pneumatic Walking Robot*. Cambridge, MA: MIT.

BLICKHAN, R. (1989). The spring-mass model for running and hopping. *J. Biomech.* **22**, 1217–1227.

BLICKHAN, R. AND FULL, R. J. (1987). Locomotion energetics of the

ghost crab. II. Mechanics of the center of mass during walking and running. *J. exp. Biol.* **130**, 155–174.

BLICKHAN, R. AND FULL, R. J. (1992). Mechanical work in terrestrial locomotion. In *Biomechanics: Structures and Systems, A Practical Approach* (ed. A. A. Biewener), pp. 75–96. Oxford: IRL Press at Oxford University Press.

BLICKHAN, R. AND FULL, R. J. (1993). Similarity in multilegged locomotion: bouncing like a monopode. *J. comp. Physiol.* A **173**, 509–517.

CAVAGNA, G. A., HEGLUND, N. C. AND TAYLOR, C. R. (1977). Mechanical work in terrestrial locomotion: two basic mechanisms for minimizing energy expenditure. *Am. J. Physiol.* **233**, R243–R261.

CAVAGNA, G. A. AND KANEKO, M. (1977). Mechanical work and efficiency in level walking and running. *J. Physiol., Lond.* **268**, 467–481.

CRUSE, H. (1976). The control of body position in the stick insect (*Carausius morosus*), when walking over uneven surfaces. *Biol. Cybernetics* **24**, 25–33.

FARLEY, C. T., GLASHEEN, J. AND MCMAHON, T. A. (1993). Running springs: speed and animal size. *J. exp. Biol.* **185**, 71–86.

FEDAK, M. A., HEGLUND, N. C. AND TAYLOR, C. R. (1982). Energetics and mechanics of terrestrial locomotion. II. Kinetic energy changes. of the limbs and body as a function of speed and body size in birds and mammals. *J. exp. Biol.* **97**, 23–40.

FULL, R. J. (1989). *Mechanics and Energetics of Terrestrial Locomotion: from Bipeds to Polypeds.* Innsbruck, Stuttgart, New York: Georg Thieme Verlag.

FULL, R. J. (1993). Integration of individual leg dynamics with whole body movement in arthropod locomotion. In *Biological Neural Networks in Invertebrate Neuroethology and Robotics* (ed. R. D. Beer, R. E. Ritzmann and T. McKenna), pp. 3–20. Boston: Academic Press, Inc.

FULL, R. J. AND AHN, A. N. (1995). Static forces and moments generated in the insect leg: comparison of a three-dimensional computer model with experimental measurements. *J. exp. Biol.* **198**, 1285–1298.

FULL, R. J., BLICKHAN, R. AND TING, L. H. (1991). Leg design in hexapedal runners. *J. exp. Biol.* **158**, 369–390.

FULL, R. J., KRAM, R. AND WONG, B. (1993). Instantaneous power at the leg joints of running roaches. *Am. Zool.* **33**, 140A.

FULL, R. J. AND TU, M. S. (1990). The mechanics of six-legged runners. *J. exp. Biol.* **148**, 129–146.

FULL, R. J. AND TU, M. S. (1991). Mechanics of a rapid running insect: two-, four- and six-legged locomotion. *J. exp. Biol.* **156**, 215–231.

FULL, R. J., YAMAUCHI, A. AND JINDRICH, D. L. (1995). Single leg force production: cockroaches righting and running on photoelastic gelatin. *J. exp. Biol.* **198**, 2441–2452.

GRAY, J. (1968). *Animal Locomotion.* London: Weidenfeld & Nicolson.

HEGLUND, N. C., CAVAGNA, G. A. AND TAYLOR, C. R. (1982*a*). Energetics and mechanics of terrestrial locomotion. III. Energy changes of the centre of mass as a function of speed and body size in birds and mammals. *J. exp. Biol.* **97**, 41–56.

HEGLUND, N. C., FEDAK, M. A., TAYLOR, C. R. AND CAVAGNA, G. A. (1982*b*). Energetics and mechanics of terrestrial locomotion. IV. Total mechanical energy changes as a function of speed and body size in birds and mammals. *J. exp. Biol.* **97**, 57–66.

HILDEBRAND, M. (1960). How animals run. *Scient. Am.* **202**, 148–157.

HIROSE, S. (1984). A study of design and control of a walking vehicle. *Int. J. Robot. Res.* **3**, 113–133.

MARTIN, P. E., HEISE, G. D. AND MORGAN, D. W. (1993). Interrelationships between mechanical power, energy transfers and walking and running economy. *Med. Sci. Sports Exerc.* **25**, 508–515.

MCMAHON, T. A. AND CHENG, G. C. (1990). The mechanics of running: how does stiffness couple with speed? *J. Biomech.* **23**, 65–78.

OKHOTSIMSKIY, D. Y., PALTONOV, A. K., BOROVIN, G. K. AND KARPOV, I. I. (1972). Digital computer simulation of the motion of a stepping vehicle. *Eng. Cybernetics* **10**, 410–419.

POWERS, A. C. (1996). *Research in the Design and Construction of Biologically-Inspired Robots*. Berkeley, CA: U. C. Berkeley.

RAIBERT, M. H. (1990). Trotting, pacing and bounding by a quadruped robot. *J. Biomech.* **23**, 79–98.

RAIBERT, M. H. AND HODGINS, J. A. (1992). Legged robots. In *Biological Neural Networks in Invertebrate Neuroethology and Robotics* (ed. R. Beer, R. Ritzmann and T. McKenna), pp. 319–354. Boston: Academic Press.

TING, L. H., BLICKHAN, R. AND FULL, R. J. (1994). Dynamic and static stability in hexapedal runners. *J. exp. Biol.* **197**, 251–269.

WILLEMS, P. A., CAVAGNA, G. A. AND HEGLUND, N. C. (1995). External, internal and total work in human locomotion. *J. exp. Biol.* **198**, 379–393.

WILLIAMS, K. R. AND CAVANAGH, P. R. (1983). A model for the calculation of mechanical power during distance running. *J. Biomech.* **16**, 115–128.